

ARTICLE

Ocular and systemic safety of a recombinant AAV8 vector for X-linked retinoschisis gene therapy: GLP studies in rabbits and Rs1-KO mice

Dario Marangoni^{1,2}, Ronald A Bush¹, Yong Zeng¹, Lisa L Wei³, Lucia Ziccardi^{1,4}, Camasamudram Vijayasarathy¹, Joshua T Bartoe⁵, Kiran Palyada^{5,6}, Maria Santos¹, Suja Hiriyanna³, Zhijian Wu³, Peter Colosi^{3,7} and Paul A Sieving^{1,3}

X-linked retinoschisis (XLRS) is a retinal disease caused by mutations in the gene encoding the protein retinoschisin (RS1) and is one of the most common causes of macular degeneration in young men. Our therapeutic approach for XLRS is based on the administration of AAV8-scRS/IRBPhRS, an adeno-associated viral vector coding the human RS1 protein, via the intravitreal (IVT) route. Two Good Laboratory Practice studies, a 9-month study in New Zealand White rabbits ($n = 124$) injected with AAV8-scRS/IRBPhRS at doses of 2E9, 2E10, 2E11, and 1.5E12 vector genomes/eye (vg/eye), and a 6-month study in Rs1-KO mice ($n = 162$) dosed with 2E9 and 2E10 vg/eye of the same vector were conducted to assess ocular and systemic safety. A self-resolving, dose-dependent vitreal inflammation was the main ocular finding, and except for a single rabbit dosed with 1.5E12 vg/eye, which showed a retinal detachment, no other ocular adverse event was reported. Systemic toxicity was not identified in either species. Biodistribution analysis in Rs1-KO mice detected spread of vector genome in extraocular tissues, but no evidence of organ or tissues damage was found. These studies indicate that IVT administration of AAV8-scRS/IRBPhRS is safe and well tolerated and support its advancement into a phase 1/2a clinical trial for XLRS.

Molecular Therapy — Methods & Clinical Development (2016) **5**, 16011; doi:10.1038/mtm.2016.11; published online 16 March 2016

INTRODUCTION

X-linked retinoschisis (XLRS) is a rare ocular disease caused by mutations in the retinoschisin gene (RS1).^{1,2} An absent or nonfunctional retinoschisin protein disrupts the retinal architecture, with splitting of retinal layers, formation of intraretinal cavities, and progressive deterioration of visual function.^{3–5} Although no approved therapy is currently available for XLRS patients, proof-of-concept studies in a murine model of XLRS demonstrated improvement of both retinal structure and function following viral mediated RS1 gene replacement^{6–11} and established the basis for testing the feasibility of a gene therapy approach in a XLRS human trial. Recently, evidence that viral vector RS1 transfer can restore synaptic function and structure in the Rs1-KO mouse provided further insights into the mechanism by which normal RS1 protein can ameliorate retinal dysfunction and further supports this approach.¹²

Our therapeutic strategy is based on administering AAV8-scRS/IRBPhRS, an adeno-associated viral vector coding the human RS1 protein, via the intravitreal (IVT) route. IVT injection is considered a safe and less invasive procedure, routinely used in the clinical practice to deliver different pharmacological agents into the human

eye and therefore, an alternative to the surgical subretinal delivery. A previous pilot study in the rabbit eye showed that IVT injection of AAV8-scRS/IRBPhRS is safe and well tolerated in the short term, as it produced only mild and transitory ocular inflammation without any irreversible tissue damage.¹³

These encouraging results supported development of two additional long-term Good Laboratory Practice (GLP) compliant safety studies in which we administered AAV8-scRS/IRBPhRS by IVT injection in two different animal species, Rs1-KO mice and New Zealand White rabbits as a prelude to developing a clinical trial.

The Rs1-KO mouse is currently the only existing animal model that recapitulates the XLRS human disease and that, conversely to wild-type animals,¹⁴ allows for efficient transduction of retinal cells by AAV8-based vectors after IVT injection.⁸ Hence, it is the only animal model that allows for assessing the immune reaction to the Rs1 transgene and the ocular and systemic distribution of AAV8 vector, given the concurrent disruption of retinal architecture induced by XLRS disease.

The rabbit was also selected because its larger vitreous humor volume and retinal surface area more closely resemble the human

The first three authors contributed equally to this work.

¹National Institute on Deafness and Other Communication Disorders, National Institutes of Health, Bethesda, Maryland, USA; ²Department of Biotechnology and Applied Clinical Science, University of L'Aquila, L'Aquila, Italy; ³National Eye Institute, National Institutes of Health, Bethesda, Maryland, USA; ⁴Current address: G.B. Bietti Foundation-IRCCS, Department of Neurophysiology of Vision and Neurophthalmology, Rome, Italy; ⁵MPI Research, Mattawan, Michigan, USA; ⁶Current address: Merck Research Laboratory, Kenilworth, New Jersey, USA; ⁷Current address: BioMarin Pharmaceutical Inc., Novato, California, USA. Correspondence: Paul A. Sieving (paulsieving@nei.nih.gov)

Received 8 November 2015; accepted 18 January 2016

eye compared with the mouse. The rabbit eye offers suitable representation of tissue exposure and dispersion of the tested article as expected in human XLR5 patients, while utilizing an identical IVT injection procedure employed in the clinic.

These two studies were undertaken to support an investigational new drug application to FDA and therefore were purposely designed to provide information that would adequately address the safety and tolerability of the lead drug candidate prior to initiating human clinical trials.

Considered together, the results of these two GLP compliant studies demonstrated that AAV8-scRS/IRBPhRS is generally well tolerated, locally and systemically, and support its advancement into a human phase-1/2a clinical trial for patients with XLR5.

RESULTS

9-month rabbit study

Ophthalmic examination. Results of ophthalmic testing in New Zealand White rabbits are summarized in Table 1. No animals receiving 2E9 vg/eye showed any pathological abnormality in either the anterior or posterior segments of injected eyes at any time point. The most common clinical finding in the treated eye of the higher vector dosing groups was the presence of multifocal, pinpoint, white precipitates in the mid-vitreous; leukocyte infiltration and accumulation was considered the most likely explanation. These were first observed at 2 weeks postinjection and their prevalence was dose dependent as they were detected in 3 animals (13%) in the 2E10 vg/eye group and in 13 (54%) and 21 animals (88%) in the 2E11 vg/eye and in the 1.5E12 vg/eye, respectively. The vitreal precipitates were transient as they resolved completely by 3 months in both 2E10 and 2E11 vg/eye groups and between 6 and 9 months in the 1.5E12 vg/eye group. Due to this pattern of observed resolution, they were considered as nonadverse events.

Less common clinical findings in treated eyes were vitreal hemorrhage or signs of anterior uveitis. Fibrin deposits adjacent to the optic nerve head were observed in one animal in the 2E11 vg/eye group at the 2-week and 3-month time points. Three animals receiving 1.5E12 vg/eye showed midvitreous clotted hemorrhage at 2 weeks postinjection. Choroidal trauma resulting from a misplaced needle insertion, not directed through the pars plana, was considered the most likely explanation for the hemorrhage. Anterior

uveitis was noted at 2 weeks in one animal (4%) in the 2E10 vg/eye group (#3004), which had cellular precipitates on the anterior lens capsule, and in two animals (8%) in the 1.5E12 vg/eye group. Of these, animal #5012 had mild iridal stromal thickening and cellular precipitates on the anterior capsule and animal #5007 showed miosis, iridal vascular injection associated with stromal thickening and aqueous humor flare. At the next examination time (3-month), animal #5012 showed an improvement of the uveitis, with reduction of stromal thickening and cellular precipitates, but inflammation had progressed in animal #5007 and resulted in multifocal iridolenticular synechiae. A total retinal detachment was observed at the 3-month time point in the latter animal. Due to the poor prognosis for ocular function, this was considered an adverse effect associated with the 1.5E12 vg/eye, highest dose tested.

Except for one animal (#5020) in the 1.5E12 vg/eye group that had an incipient, axial, subcapsular, lenticular opacity in the uninjected eye at the 3-month time point, no other abnormality was reported in the uninjected eye for all the duration of the study. Since the lens opacity in animal #5020 did not progress at subsequent 6 and 9-month time-points, it was considered incidental and suspected to be a breed-related change.

Intraocular pressure (IOP). Mean IOP values by group were within the range of expected values at all time points during the study, ranging from 11.1 ± 2.5 to 15.7 ± 2.7 mmHg for the injected eye and 11.3 ± 2.4 to 15.5 ± 3.0 mmHg for the uninjected eye. At 2 weeks, the IOP interocular ratio (treated eye/untreated eye) of rabbits in the 1.5E12 vg/eye was significantly reduced with respect to controls indicating a decrease in IOP in the injected eye, probably induced by the release of inflammatory mediators consequent to the intraocular inflammation. No other statistically significant differences in IOP interocular ratio were found between different treatment groups at any tested time point. (see Supplementary Figure S1)

Retinal electrophysiology. Retinal toxicity was also assessed by electroretinography (ERG) (Figure 1). Scotopic and photopic ERGs were recorded at baseline and at 2 weeks, 3 and 9 months after treatment. No statistically significant differences in ERG amplitude interocular ratio (treated eye/untreated eye) were found between different treatment groups at any time point tested, indicating that the injection of AAV8, at the tested doses, did not affect

Table 1 Ophthalmic examination findings in New Zealand White rabbits

Treatment	Baseline	2nd day	2nd week	3rd month	6th month	9th month
Vehicle	(0/28)	(0/28)	(0/28)	(0/21)	(0/13)	(0/7)
AAV8-vector (2E9 (vg/eye))	(0/24)	(0/24)	(0/24)	(0/18)	(0/12)	(0/6)
AAV8-vector (2E10 (vg/eye))	(0/24)	(0/24)	Anterior uveitis (1/24) Vitreous precipitates (3/24)	(0/18)	(0/12)	(0/6)
AAV8-vector (2E11 (vg/eye))	(0/24)	(0/23)	Corneal epithelial peeling (1/24) Vitreous precipitates (13/24)	(0/18)	(0/12)	(0/6)
AAV8-vector (1.5E12 (vg/eye))	(0/24)	Vitreous hemorrhages (1/23)	Anterior uveitis (3/24) Vitreous precipitates (21/24) Vitreous hemorrhages (3/24)	Anterior uveitis (2/18) Retinal detachment (1/18)	Vitreous precipitates (1/11)	(0/6)

Ophthalmic abnormalities in the injected eye are reported as observed number by total number of animals. Except for one rabbit in the 1.5E12 vg/eye group that had an incipient, axial, subcapsular, lenticular opacity in the uninjected eye at 3-month time point, no other abnormality was reported in the uninjected eye for the duration of the study.

retinal function in the treated eyes on average. All ERG amplitudes were within normal limits for all animals at all time points with the exception of animal #5007. This animal developed a retinal detachment by the 3-month time point when the ERG scotopic and photopic b-wave amplitudes were both reduced by 65% in the treated eye compared with untreated eye.

Ocular histopathology. AAV8-scRS/IRBPhRS-related histopathological findings were limited to the injected eye and consisted of a dose-dependent ocular inflammation that was greater at the 2-week time point and decreased substantially at the subsequent intervals.

At the 2-week time point, the main histopathological finding was the presence of vitreous inflammation consistent with the *in vivo* ophthalmic examination finding of vitreal precipitates. Inflammatory infiltrates consisted of variable proportions of lymphocytes, plasma cells, and macrophages, and were associated in some animals with eosinophilic proteinaceous fluid. Vitreous inflammation was observed in all AAV8 vector dose groups, with severity from minimal to severe and it was dose related, as shown by a greater prevalence of larger infiltrate in the higher dose groups (Figure 2). Minimal to mild inflammation was also observed in the optic nerve head and in the ganglion cell layer of peripapillary retinal areas.

Variable degrees of inflammation, ranging from minimal to moderate, were also observed in the anterior segment of treated eyes and involved the limbus, the filtration angle, the iris, and the ciliary body. The inflammatory reaction in the anterior segment was

detected almost exclusively in the 2E10, 2E11, and 1.5E12 vg/eye dose groups, since only a single animal in the 2E9 vg/eye showed minimal inflammation in the ciliary body.

By 3 months postinjection, the inflammation in both the anterior and the posterior segment was markedly reduced or resolved. At 9 months, residual vitreal inflammation, classified as mild and minimal, was only detectable in the 2E11 and 1.5E12 vg/eye groups and except for three rabbits in the 1.5E12 vg/eye dose group with minimal inflammation in the ciliary body, no other animal showed inflammatory infiltrates in the anterior segment.

It is worth noting that this study used a more sensitive grading system with a low threshold for the inflammatory cells for each severity category, ranging from <100 cells (minimal) to >500 cells (severe). Typical grading systems for inflammation in other organs and, in general, for ocular studies classify minimal inflammation based on the presence of less than 500 inflammatory cells. Based on this, all the inflammation graded in different compartments of the eyes in this study would be categorized under minimal, except the inflammation in the vitreous chamber in some animals at the 2-week interval.

Neutralizing antibodies (NABs) against AAV8 capsid, antibodies against transgene product, and serum transgene (RS1) levels. No animal showed preexisting NABs to AAV8 prior to administration of vehicle or AAV8-scRS/IRBPhRS. Injection of AAV8-scRS/IRBPhRS generated a dose-dependent increase in Nab production that was first observed and peaked in the majority of animals at 2

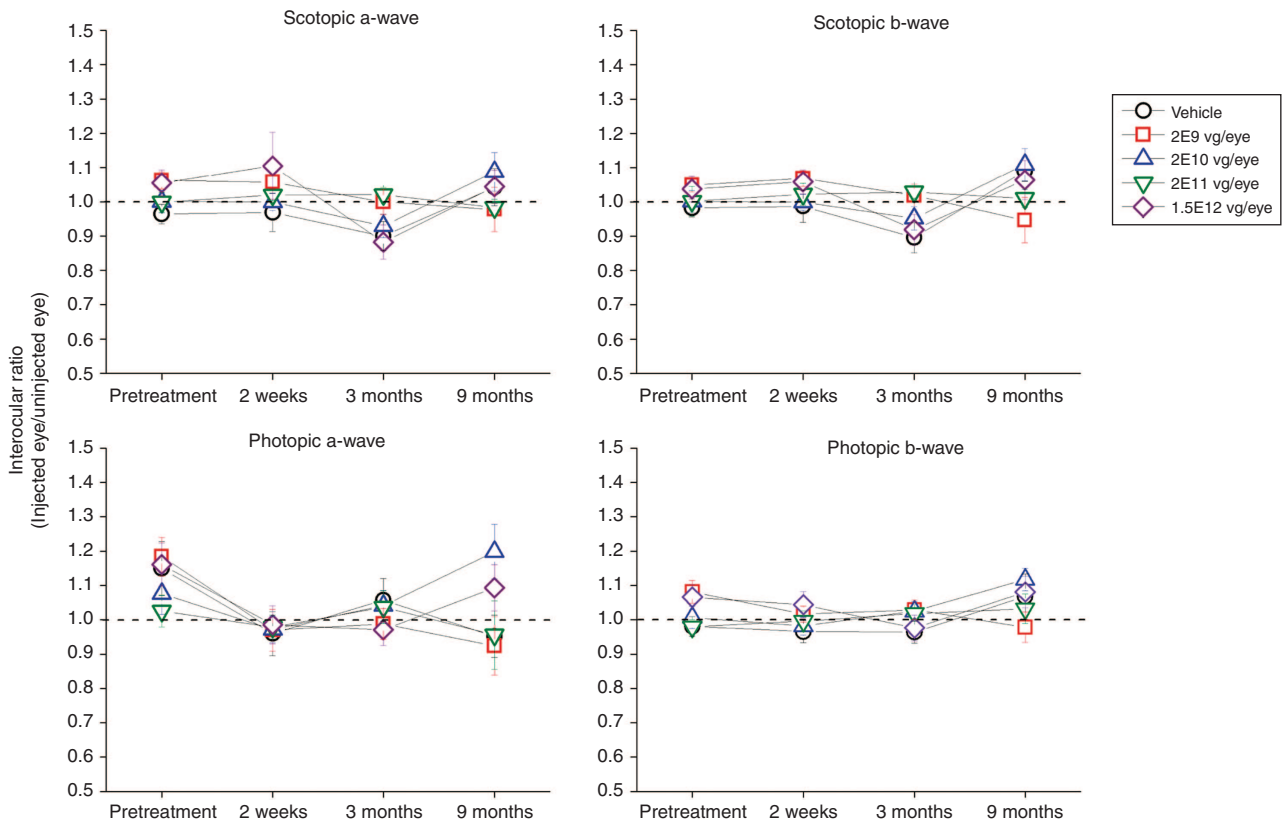


Figure 1 Electroretinogram (ERG) amplitudes in New Zealand White rabbits intravitreally injected with four doses (2E9, 2E10, 2E11, and 1.5E12 vg/eye) of AAV8-scRS/IRBPhRS and vehicle. The mean \pm SE interocular ratios (injected eye/uninjected eye) of the scotopic and photopic a- and b-wave amplitudes are shown at four time points (pretreatment, 2 weeks, 3, and 9 months after injection) for all vector doses and vehicle. A ratio equal to 1, evidenced by the black dotted line, indicates no difference between the amplitude in the treated versus the untreated eye. No significant difference in ERG amplitude was found between rabbits which received vehicle or any vector dose at all the tested time points.

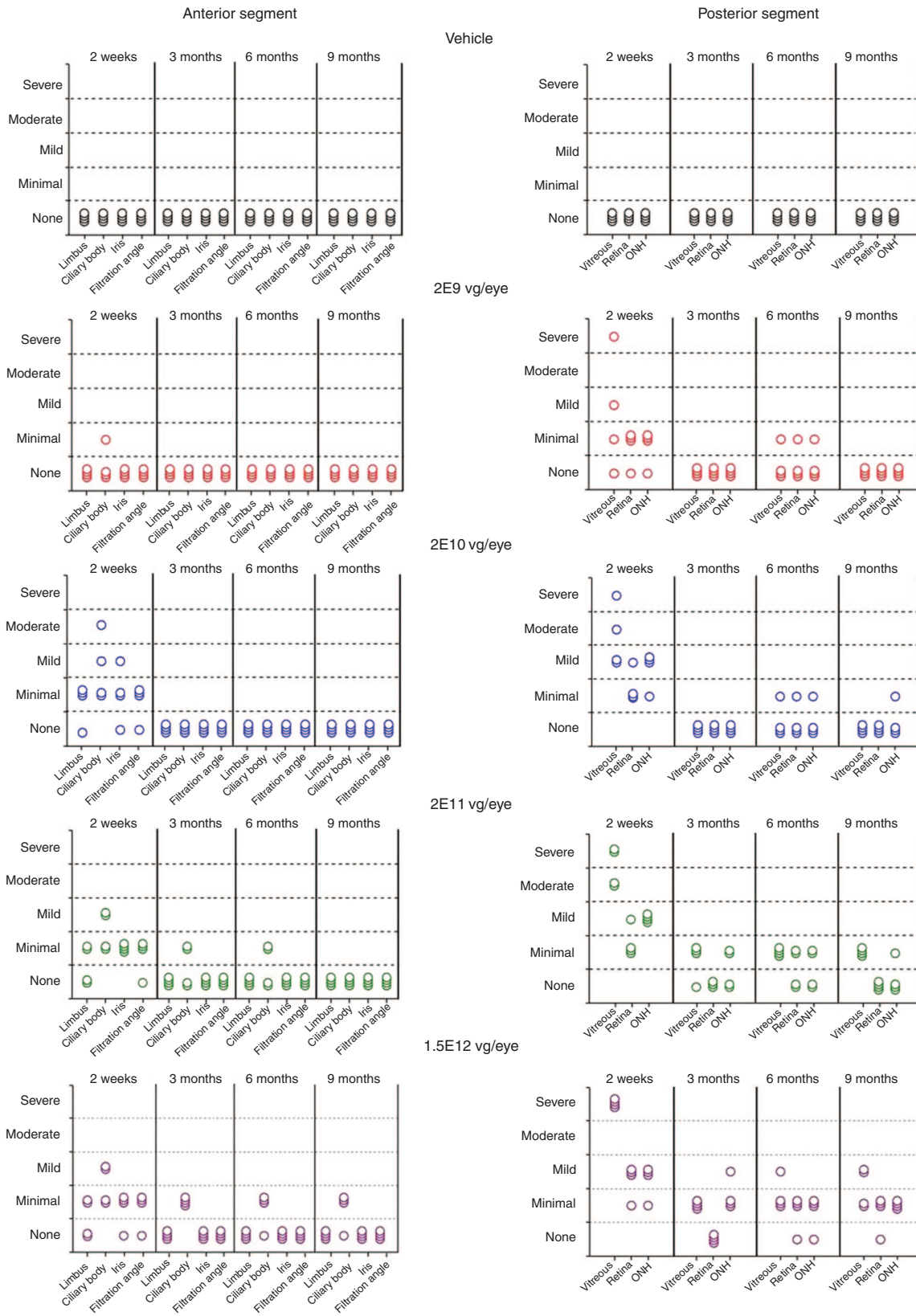


Figure 2 Histopathological grading of ocular inflammation in New Zealand White rabbits intravitreally injected with four doses (2E9, 2E10, 2E11, and 1.5E12 vg/eye) of AAV8-scRS/IRBPhRS and vehicle. Findings from the injected eye are displayed for each animal at four time points (2 weeks, 3, 6, and 9 months postinjection). The severity of the inflammatory reaction in different eye compartments was graded according to the number of inflammatory cells and classified as follows, *minimal* <100 inflammatory cells, *mild* 100–250 inflammatory cells, *moderate* 250–500 inflammatory cells and *severe* >500 inflammatory cells. Each symbol in the figure represents a single animal.

weeks (see Supplementary Table S1). At the two highest doses of AAV8-scRS/IRBPhRS (2E11 and 1.5E12 vg/eye), the majority of animals showed high levels of AAV8 capsid NABs at 2 weeks that remained high until the end of the study at 9 months. Vehicle administration produced no AAV8 capsid NABs at any time point. No RS1 antibody was detected in the rabbit serum at any AAV8-scRS/IRBPhRS vector dose. The transgene product RS1 was also not detected in the serum samples collected at any time point.

Vector biodistribution. Dose-dependent levels of vector DNA were found in the vitreous humor of the injected eye 2 weeks after treatment (Figure 3a). In all dosing groups, the vector concentration within the vitreous decreased substantially at 3 and 6 months and then remained relatively steady at a low level from 6 to 9 months. At 9 months, both 2E11 and 1.5E12 vg/eye groups showed persistence of higher levels of vector DNA in comparison to lower doses.

Only the 1.5E12 vg/eye group showed quantifiable copies of AAV8-scRS/IRBPhRS in the vitreous of the uninjected eye. These were detected at 2 weeks and 3 months postinjection and by 6 months all vitreous samples were negative.

Quantifiable copies of AAV8-scRS/IRBPhRS in the serum were detected at 2 weeks postinjection in rabbits which were dosed with 2E11 and 1.5E12 vg/eye. Vector genomes completely cleared from the serum by 3 months (Figure 3b).

Peripheral blood leukocyte analysis. Peripheral blood mononuclear cell (PBMC)-mediated proliferation profiles after stimulation with the three separate AAV8 peptide pools (PP) were at equivalent levels to PBMCs treated with the negative control, across all intervals and dosage groups, indicating that none of the three AAV8 PP induced a peripheral blood T-cell immune response (see Supplementary Figure S2). Positive control *in vitro* stimulation with concanavalin A for all samples did induce a PBMC-proliferative response, indicating that the cytometry assay was robust enough to detect a positive signal.

Body weights and food consumption. There were no test article-related changes in mean body weights or mean food consumption values across groups. Mean food consumption decreased for 2E11 and 1.5E12 vg/eye groups at week 27 (16 and 20%, respectively), compared with controls, but there were no corresponding decreases in group mean body weight values compared with controls at these intervals. Therefore, this change was not considered as test article related.

Mortality and physical observation. Except for one animal in the control group that was euthanized on day 179 due to declining health status and decreased body weight and food consumption, all rabbits remained clinically healthy for the duration of the study.

Clinical pathology. There were no test article-related effects among hematology parameters (see Supplementary Figure S3), coagulation times, fibrinogen values (see Supplementary Figure S4), and clinical chemistry analytes (see Supplementary Figure S5) in any treatment group. All mean and individual values were considered within expected ranges for biological and/or procedure-related variation despite occasional mean values that reached statistical significance.

Organ pathology. There were no test article-related macroscopic findings at scheduled necropsies in any examined organs (other than eye as previously described) and no test article-related changes in the organ weights in any dose group during the study.

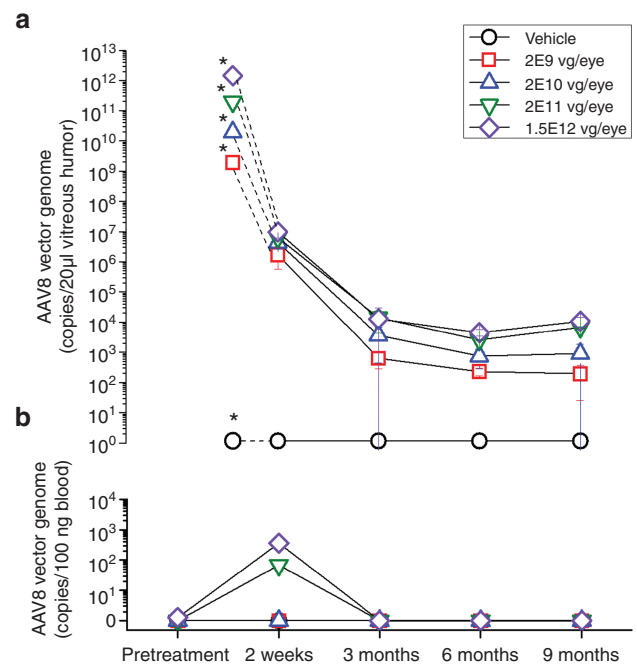


Figure 3 Biodistribution of AAV8-scRS/IRBPhRS in the vitreous humor and blood of New Zealand White rabbits injected with four doses (2E9, 2E10, 2E11, and 1.5E12 vg/eye) of AAV8-scRS/IRBPhRS and vehicle. The mean ± SD copy numbers of AAV8-scRS/IRBPhRS DNA in the vitreous humor of the injected eye (a) and blood (b) of New Zealand White rabbits are shown at five time points (pretreatment, 2 weeks, 3, 6 and 9 months after injection) for all vector doses and vehicle. Pretreatment vector DNA copy numbers in the rabbit vitreous were not assayed and the values marked by an asterisk correspond to the number of vector genomes which were injected into the vitreous. Copy numbers of AAV8-scRS/IRBPhRS are reported as copies/20 µl vitreous humor or copies/100 ng blood.

6-month Rs1-KO mouse study

Ocular examination. No mice showed any abnormality in the injected eye at baseline screening (see Supplementary Table S2). After treatment, the main ocular abnormality in injected eyes was the presence of small chorioretinal lesions. These consisted of single, well-delineated regions of altered pigmentation (<1 optic disc diameter) affecting the retina and/or choroid and associated with adjacent hemorrhages in some animals. These lesions were considered to have most likely resulted from the injection procedure, as they were evenly distributed across all the three treatment groups and in proximity to the expected injection site in the nasal and inferior retinal quadrants. Chorioretinal lesions were described in 85% of animals by 1 or 3 days after injection and were observed in the remaining 15% at 1-month follow-up.

Some treated eyes showed lens opacities. These were classified as incipient (affecting <15% of the lens fibers) and involved the posterior capsule and/or the posterior cortex. Lens opacities were observed in three animals injected with the vehicle, and in one mouse in the 2E9 vg/eye group. These lenticular opacities were considered most likely secondary to the original injection procedure.

Except for one mouse in the 2E9 vg/eye group with a diffuse corneal opacity in the untreated eye at baseline that remained unchanged throughout duration of the study, no other mouse showed any abnormality in the untreated eye during the study.

Ocular histopathology. No AAV8-scRS/IRBPhRS-related findings were reported in the mouse study. Significant histopathological abnormalities (Figure 4) were limited to the injected eye and were

present in all the treatment groups including the control, with no dose-dependent difference in the incidence/severity across treatment groups. Hence these findings were attributed to the injection procedure.

An inflammatory reaction characterized by lymphocytes and macrophages was reported at the limbus in most animals and frequently extended to the adjacent cornea and into extraocular structures along the outer aspect of the conjunctiva and bulbar muscles. Other findings included proteinaceous fluid (eosinophilic granular material) in the anterior chamber and hemorrhage and proteinaceous granular material within the vitreous chamber. Compared with day 3, there was a significant decrease in the prevalence/severity of these findings at 1 month with a complete resolution at 6 months.

NABs against AAV8 capsid, antibodies against transgene product, and plasma transgene (RS1) levels. All animals in the 2E9 vg/eye dose group had negligible (below 1:50) titers of NABs against AAV8 capsid during the 6-month period. In the 2E10 vg/eye dosing group, 67% of the animals showed NAB titers higher than 1:50 at 180 days (see Supplementary Table S3). No animals in the vehicle control group

had measurable NAB titers to AAV8. No antibodies were detected to the transgene product RS1 in any of the tested plasma samples and none of the plasma samples showed presence of the transgene protein RS1.

Biodistribution and RS transgene expression. Biodistribution of AAV8-scRS/IRBPhRS vectors in mouse tissues was assayed by quantitative PCR (qPCR) analysis in the blood and in relevant organs collected from each mouse at 3-day- and 6-month postvector administration (Figure 5a). The following tissues were analyzed from each animal: left (only two animals from each group on day 3) and right gonads, right epididymis, lung, heart, kidney, spleen, liver, left (only animals on day 3) and right brain, left eye, left optic nerve, optic chiasm, right mandibular lymph node, right lacrimal gland, right harderian gland, right optic nerve, and right eye.

At 3 days, vector was detected in the blood and in all the analyzed tissues of all the Rs1-KO mice in the 2E9 and 2E10 vg/eye group. Some animals showed copy number below the limit of quantitation in the left optic nerve (4 out of 10), in the optic chiasm (3 out of 10), in the gonads (4 out of 10) and in the epididymis (1 out of 9), but all the other mice had quantifiable levels of AAV8-scRS/IRBPhRS

Main histopathological findings in Rs 1-KO mice

	3 days			1 month			6 months		
	Vehicle n = 12	2E9 n = 12	2E10 n = 12	Vehicle n = 12	2E9 n = 12	2E10 n = 12	Vehicle n = 12	2E9 n = 12	2E10 n = 12
Limbus inflammation	4 ^{Min} 1 ^{Mild}	3 ^{Min} 4 ^{Mild}	6 ^{Min} 2 ^{Mild}	1 ^{Min}	3 ^{Min}	3 ^{Min}	0	0	0
Proteinaceous fluid in the AC	2 ^{Min} 2 ^{Mild}	0	1 ^{Min} 1 ^{Mild}	0	0	0	0	0	0
Vitreous hemorrhage	1 ^{Min}	2 ^{Min}	1 ^{Min} 1 ^{Mod}	1 ^{Min}	0	0	0	0	0

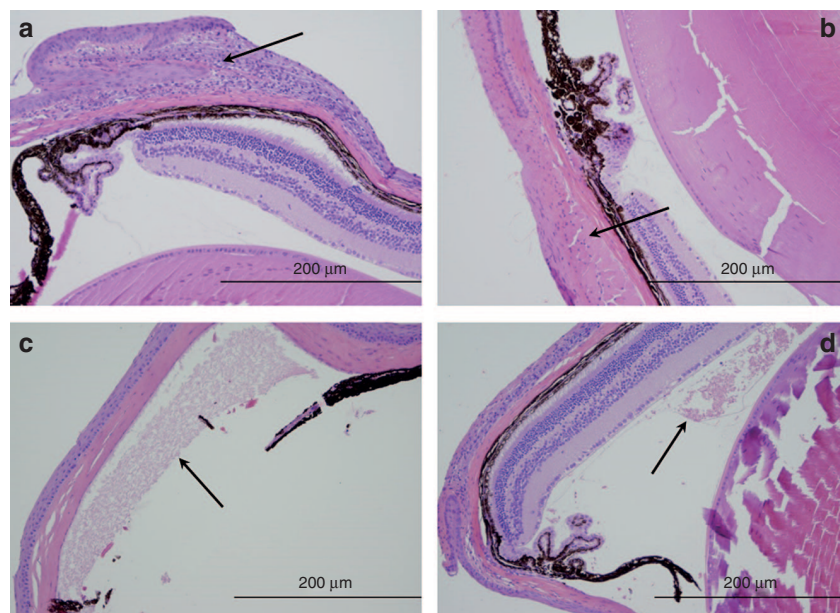


Figure 4 Main histopathological findings in Rs1-KO mice intravitreally injected with AAV8-scRS/IRBPhRS at 2E9 and 2E10 vg/eye and vehicle. At 3 days after injection, a variable number of inflammatory cells were detected at the limbus of the injected eye of Rs1-KO mice treated with vehicle and with both 2E9 and 2E10 (a, arrow) vg/eye doses of AAV8-scRS/IRBPhRS. At 6 months, the limbal inflammation completely resolved in all groups, including the 2E10 vg/eye dose group (b, arrow). Some animals from each treatment group showed proteinaceous fluid deposits in the anterior chamber (c, arrow), and hemorrhages in the vitreous chamber, mainly at 3 days after injection. (d, arrow). All the described findings were attributed to the injection procedure. The inflammatory cells were counted and graded as *minimal* (<25), *mild* (25–50), *moderate* (50–75) and *severe* (>75). Hemorrhage was classified according to the number of red blood cells as *minimal* (<50), *mild* (50–100), *moderate* (100–150) and *severe* (>150). Presence of proteinaceous fluid was assessed and quantified as *minimal*, *mild*, *moderate* and *severe*. Hematoxylin and eosin; Bar = 200 μm (a–d). AC, anterior chamber.

vector in the blood and in all other analyzed tissues. The highest concentrations of vector were found in the injected eye followed by liver, and by the harderian gland, mandibular lymph node and optic nerve ipsilateral to the injected eye. A comparison between the two vector doses for the same tissue revealed greater concentration of AAV8-scRS/IRBPhRS vector DNA in the higher dose group (2E10 vg/eye) compared with the low dose group (2E9 vg/eye).

At 6 months, the concentration of AAV8-scRS/IRBPhRS was considerably reduced in the blood of all the dosed animals. Copies of vector DNA were not detectable in the blood of the 2E9 vg/eye group and were quantifiable in the blood of a single mouse in the 2E10 vg/eye group. Except for the optic nerve contralateral to the treated eye which tested negative in two animals dosed with 2E10 vg/eye, all the other tissues showed quantifiable levels of AAV8-scRS/IRBPhRS, but most showed a decrease in vector concentration compared with 3 days.

Figure 5b shows analysis of transgene expression in relevant organs. At 3-day postinjection, four out of five liver samples in the 2E10 vg/eye group showed copy numbers of human RS transcript below limit of quantitation. All other samples in both dosing groups tested negative. At 6 months posttreatment, four out of five liver samples in the 2E9 vg/eye group tested positive for human RS transcript, but only one showed quantifiable copy numbers. In the 2E10 vg/eye dose group, quantifiable copy numbers of RS gene transcript were detected in all five liver samples and in one harderian gland ipsilateral to the injected eye.

Peripheral blood leukocyte analysis. After *in vitro* stimulation with the three separate AAV8 PP, T cell-mediated IFN γ + percentage values

were at the same levels as splenocytes treated with the negative control, indicating that none of the three AAV8 PP and RS-1 antigen induced a T cell-mediated IFN γ + response (see Supplementary Figure S6). Positive control *in vitro* stimulation with PMA and ionomycin for all samples induced T cell-mediated IFN γ + responses in both CD4 and CD8 T cells cellular populations, indicating that the cytometry assay was robust enough to detect a positive signal.

Body weights and food consumption. Neither mean body weight nor mean food consumption showed test article-related changes for the entire duration of the study. Changes in body weights as well as in food consumption were within the range of normal biologic variability that are commonly observed in laboratory housed mice of this age.

Clinical pathology. There were no test-article related effects among hematology parameters and clinical chemistry analytes in any treatment group (see Supplementary Figure S7). Mean and individual values were within expected ranges for biological and/or procedure-related variation despite occasional mean values that reached statistical significance. Animals at 6 months receiving 2E10 vg/eye had mild increases in neutrophils, relative to controls. These findings were considered incidental and within expected ranges for animals of this species and strain on a study of this length. Furthermore, no changes in neutrophils were seen at earlier time points, nor were there other correlative study findings to suggest these fluctuations were meaningful.

Organ pathology. There were no test article-related macroscopic findings at scheduled necropsies in any of the examined organs

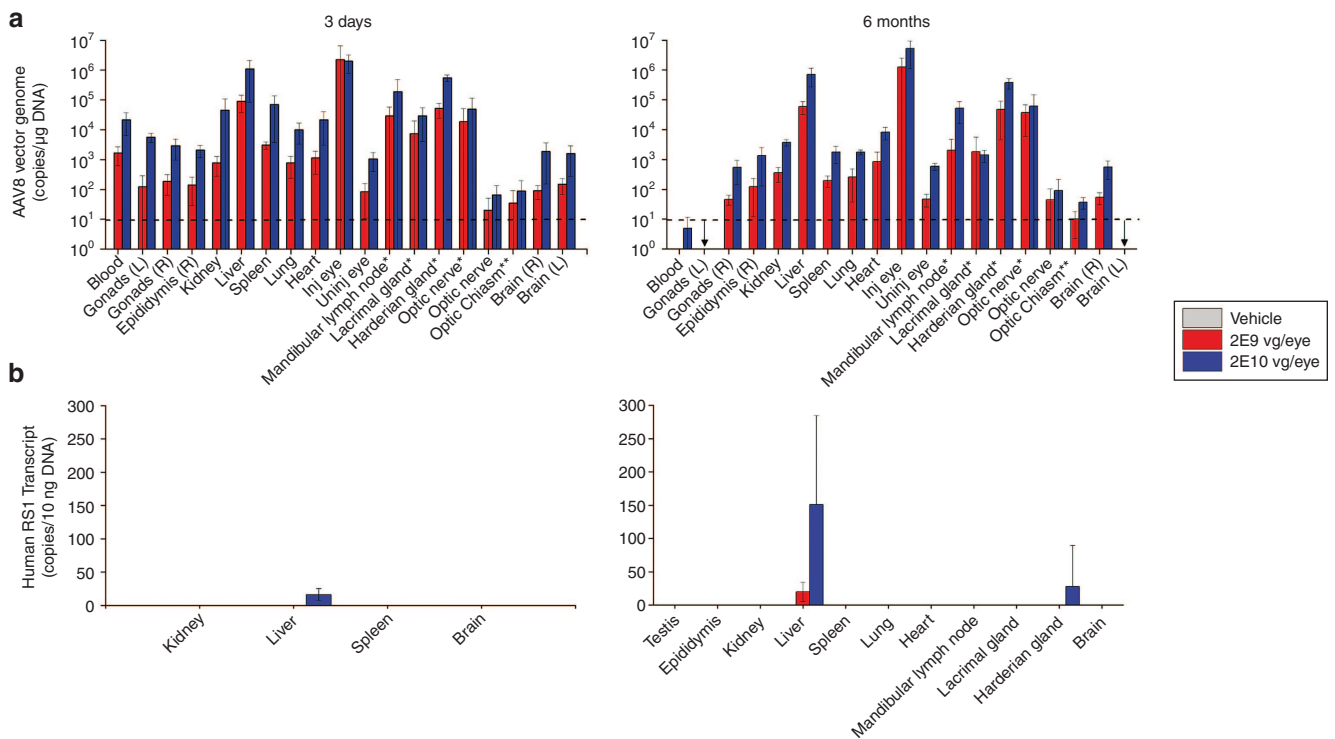


Figure 5 AAV8-scRS/IRBPhRS biodistribution and transgene expression analysis in Rs1-KO mice. **(a)** For biodistribution analysis, tissues were harvested, total DNA prepared, and AAV DNA quantified by Taq-Man qPCR analysis. The results compare vector genome copy number after intravitreal injection of vehicle and AAV8-scRS/IRBPhRS at two doses, 2E9 and 2E10 vg/eye in tissues collected at day 3 and 6 months. Copies of AAV8 genomic DNA are reported as copies per 10 µg of DNA and shown as mean \pm SD from 5 Rs1-Ko mice. Due to a contamination problem, which was later resolved, 2 vehicle treated mice at 3-day tested positive to vector DNA and were discarded. **(b)** For RS1 transgene analysis, total RNA was isolated from selected tissues, reverse transcribed to cDNA and quantified by Taq-Man based qPCR assay. Copies of human RS transcript are reported as copies per µg of cDNA and shown as mean \pm SD. *Ipsilateral to the injected eye. The arrow indicates that results from the samples were not available. Dotted lines indicate the lower limit of quantitation for vector genome copies.

(other than eye as previously described) and no test article-related changes in the organ weights of any dose group during the study.

DISCUSSION

Results from these two studies conducted under GLP conditions show that IVT injection of AAV8-scRS/IRBPhRS is safe and well tolerated in normal rabbits and in a mouse model of XLR5. Our previous 3-month safety study in rabbits¹³ tested the local ocular safety of IVT injection of AAV8-scRS/IRBPhRS at the doses of 2E10 and 2E11 vg/eye and demonstrated absence of ocular adverse events in the injected eyes at both doses. In the present rabbit GLP study, we extend this observation with evidence that dosing 2E11 vg/eye of AAV8-scRS/IRBPhRS does not lead to any functional or structural ocular damage, or systemic toxicity for up to a 9-month period.

Following the IVT injection of AAV8-scRS/IRBPhRS, the rabbits mounted a transient ocular inflammatory response that was mainly localized to the vitreous humor. Multifocal vitreal precipitates were observed clinically at 2 weeks in all dosing groups and resolved completely by 3 months at all vector doses, except for rabbits treated with 1.5E12 vg/eye in which they resolved by 9 months. Histopathological evaluation provided evidence supporting the inflammatory nature of these precipitates, showing the presence of inflammatory cells admixed with proteinaceous material in the vitreous of the vector injected eyes. Ocular inflammation was not itself considered an adverse event, as it resolved and left no evidence of any irreversible tissue damage or ERG abnormality in all but a single rabbit in the 1.5E12 vg/eye group which developed a retinal detachment at 3 months.

The occurrence of a local inflammatory reaction after intraocular administration of AAV vectors has been previously reported.^{15–18} Transient vitreal inflammation, that resolved by 3 months from administration, was described in one out of three nonhuman primates after IVT injection of 2.46 E10 vg of scAAV2-P1ND4v2, a gene therapy vector to treat Leber Optic Neuropathy in humans.¹⁸ Maclachan *et al.* evaluated the safety of an AAV2 vector expressing sFLT01, an antivascular endothelial growth factor for the treatment of age-related macular degeneration in nonhuman primates, and found that IVT administration of AAV2-sFLT1 at the dose of 2.4 E10 vg/eye induced a mild to moderate ocular inflammation that resolved in the majority of cases by 5 months, but persisted at low levels for up to 15 months in some animals.¹⁶

AAV8 capsid was considered to be the causative agent of the inflammation in this study. In our previous non-GLP study, we reported that AAV8-scRS/IRBPhRS and the AAV8 vector not expressing the RS1 transgene (AAV8-null vector) caused comparable levels of ocular inflammation.¹³ Here, we report that AAV8 capsid induced the production of NABs in both rabbits and the Rs1-KO mice, whereas no humoral response was detected against the Rs1 transgene. Consistent with the absence of significant permanent ocular tissue damage, the AAV8 capsid and the RS1 did not induce a cellular immune response indicating the lack of a cytotoxic immune reaction against vector infected cells.

Unlike in the rabbit, IVT injection of AAV8-scRS/IRBPhRS in the mouse did not cause any significant ocular inflammatory response or adverse event, at either 2E9 or 2E10 vg/eye. Since neither the rabbit nor the mouse showed preformed NABs against AAV8 capsid, and therefore any previous immunity against the AAV8-vector, the absence of an inflammatory reaction in the mouse might be due to species-specific differences in the reactivity/tolerance of the ocular immune system. Alternatively, a faster clearance of the AAV8-vector from the murine vitreous humor or its ability to penetrate the

Rs1-KO retina may also play a role in the difference between the ocular immune response in the rabbit and in the mouse. AAV8 can penetrate the Rs1-KO retina and be internalized by the retinal cells,⁸ perhaps reducing vector exposure to the immune system. Since AAV8 vector shows a weak penetration of the wild-type retina,¹⁴ vector particles would persist in the vitreous and could trigger an adaptive immune reaction. Consistent with this hypothesis, both the intensity and the time course of the vitreous inflammation in the rabbit were associated with the concentration and clearance of the vector from the vitreous. Higher doses of vector were associated with more inflammatory cells in the vitreous at 2 weeks, and as demonstrated in the biodistribution analysis, the drop in vector concentration at 3 months corresponded to a substantial reduction in the number of inflammatory cells in the vitreous. The persistence at 9 months of residual low levels of inflammatory cells in the vitreous of animals dosed with 2E11 and 1.5E12 vg/eye is likely a consequence of persistence of minimal amount of vector copies in the vitreous, sufficient to trigger a subtle but detectable ocular immune response.

Unexpectedly, IVT administration resulted in high levels of AAV8 vector genomes being detected in extraocular organs. Reflux from the needle incision has been described as a possible occurrence associated with IVT injection procedures in humans.¹⁹ Due the technical challenges associated with IVT injection in the small mouse eye, it is possible that a larger portion of the vector load flowed out of the vitreous and onto the ocular surface, transited the nasolacrimal drainage, and gained access to the systemic circulation through the highly vascularized nasal mucosa where lacrimal fluid is reabsorbed.²⁰ It is relevant to note, however, that despite a considerable amount of vector being detected outside the eye, no macroscopic or microscopic organ abnormalities were observed in the mouse or in the rabbit, even at the highest vector doses.

Analysis of transgene expression in the Rs1-KO mouse showed very low levels of RS1 transcript in the liver and in the hardier gland of mice injected with 2E10 vg/eye. In the liver, which was the organ with the highest RS1 transgene expression, a mean copy number of 150/10 ng of mRNA was detected. Based on the weight (1.34 g) and the number of hepatocytes in the mouse liver (~1.35E8), this corresponds to ~0.05 transgene copies/cell, a negligible amount considering that 5–10 copies of transcript/cell are usually considered low. In order to prevent undesired expression of RS1 transgene in extraretinal tissues, our vector is provided with a retina-specific retinoschisis promoter. Since the liver and the hardier gland were the two extraocular tissues outside the injected eye with the largest numbers of vector genomes, it may be that the vector concentration in these tissues was high enough to elicit transgene expression, albeit minimal, perhaps triggered by a low level activity of the RS1 promoter.

Our earlier studies provided proof of efficacy that our gene therapy approach to administer AAV8-scRS/IRBPhRS into the vitreous humor represents a promising strategy for the treatment of XLR5 disease. The present GLP studies provide evidence that the clinical vector, AAV8-scRS/IRBPhRS, is well tolerated and satisfies essential safety requirements necessary for advancement of this gene therapy vector into a phase 1/2a clinical trial in XLR5 patients.

MATERIALS AND METHODS

Animals and study design

Normal New Zealand White male rabbits ($n = 124$, age: ~ 6.5 months at injection; weight: 2.8–3.7 kg) and Rs1-KO mice ($n = 162$, age: 3–18 weeks at injection, weight: 12.1–26.1 g) were studied under GLP-compliant protocols. All animal studies were approved by the MPI Research Institutional

Review Board and by the Animal Care and Use Committee of the National Eye Institute. Study designs are illustrated in Tables 2 and 3.

Vector description and dosing

AAV8-sCRS/IRBPhRS delivers a self-complementary vector genome that contains a modified human retinoschisin promoter, an interphotoreceptor retinoid-binding protein (IRBP) enhancer, an intact human retinoschisin cDNA with a truncated first intron located in its authentic position between the exon 1 and 2 sequences, and a human beta-globin 3' untranslated region and polyadenylation site. This vector is packaged into an AAV serotype 8, a vector that transduces retinal cells in the Rs1-KO mice very efficiently following IVT injection.⁹ GLP manufactured material for toxicology studies was produced and analyzed at The Children's Hospital of Philadelphia in the Clinical Vector Core for the Center for Cellular and Molecular Therapeutics.

The vector doses tested in these studies were selected on the basis of data from previous efficacy studies in Rs1-KO mice (Bush *et al.*, manuscript submitted) and the maximum achievable doses in each species. For the rabbit, we used factors of 100 and 1000 to scale up from the minimum effective dose of 1E8 vg/eye in the mouse eye to equivalent doses in the human eye. These factors are the differences between mouse and human in retinal surface area and vitreal volume, respectively. Thus, 2E10 and 2E11 vg/eye were in the middle of the dosing range in the rabbit study. We then chose additional doses 1 log unit higher, also the maximum achievable dose, and one log unit lower to encompass a range we predicted would allow us to observe minimal to maximal ocular and systemic reaction to the vector. The maximum achievable dose in the mouse is 2E10 vg/eye, and, based on experience in the previous efficacy study, one log unit lower was predicted to show minimal toxicity with maximal retinal transduction. The 10-fold dose range would allow investigation of a dose effect on biodistribution in an animal model of the disease.

IVT injection

In rabbits, vector solution or vehicle was administered in the right eye by IVT using a ½ cc U-100 insulin syringe (B-D #329461) with attached 28 gauge needle. Rabbits were anesthetized with isoflurane to effect. Proparacaine hydrochloride 0.5% (2 drops) was applied to each eye. The eyelids and surrounding skin were gently swabbed using a 1:20 dilution of ophthalmic povidone iodine solution (5%) in saline. A clear, adhesive plastic drape was affixed to cover the eyelids and periocular region and a wire eyelid speculum was inserted through a slit in the drape to retract the eyelids. The intended injection site was marked 2.0mm posterior to the limbus in superotemporal quadrant with a Jamison caliper (tips previously brushed with a sterile surgical marking pen). Ophthalmic povidone-iodine solution (5%) was applied with a cotton-tipped swab to the conjunctival surface overlying the injection site. The eye was flushed with a balanced salt solution (BSS) to remove the povidone-iodine solution following appropriate contact time. The needle was advanced obliquely (to avoid lens contact) through the conjunctiva and sclera overlying the pars plana and 50 µl of vehicle was injected into the midvitreal of the right eye. Thirty seconds was allowed to elapse prior to removal of the injection needle to ensure distribution of the injected solution with minimal subsequent reflux through the resultant sclerotomy site. The eyelid speculum and drape were removed. An identical procedure was performed on the left eye except 50 µl of vehicle was injected instead. Immediately following bilateral injection, animals were subjected to slit-lamp biomicroscopy and indirect ophthalmoscopy to verify the eyes had experienced no trauma during ocular preparatory procedures or IVT. Neomycin/polymyxin B/bacitracin ophthalmic ointment was placed into both eyes of each animal following ocular examination.

In Rs1-KO mice, the vehicle or test article was administered once via IVT injection into the right eye. Animals were anesthetized with a ketamine and xylazine cocktail given intraperitoneally (80 and 10 mg/kg, respectively). Supplemental doses of anesthesia were administered (via intraperitoneal injection) to achieve or maintain the anesthesia plane as needed. One drop of 0.5% tetracaine was applied topically to the corneal surface of the right (dosing) eye. A sterile artificial tears ointment was applied to the corneal surface of the left/nondosing eye to minimize postinjection cataracts. The syringes were loaded at the time of injection. Using a 10-µl Nanofil syringe (World Precision Instruments, Sarasota, FL) with a removable 35 gauge needle, animals were injected under a dissecting microscope with 1 µl of test article or vehicle into the vitreal body through the nasal side of the right eye approximately 1 mm posterior to the limbus. The needle was carefully placed beside the lens to avoid damaging it. Following administration of the material, the needle was carefully withdrawn from the eye. Neomycin/polymyxin B/bacitracin ophthalmic ointment was applied to the injection site.

The needle was reused for mice in the same dosing group until it was dull. A new syringe was used for each dosing group. The mice were placed onto a circulating warm water blanket while recovering from the anesthesia and were placed back into cages when recovered. Antisedan[®] was administered subcutaneously, intraperitoneally, or intramuscularly as a sedation reversal agent. Animals were also given lactated ringers solution subcutaneously during recovery from anesthesia as needed to help with dehydration. Diet Gel[®], Enviro-dri[®], and supplemental heat were offered as needed.

Ophthalmic examination and ERG

A board-certified veterinary ophthalmologist (J.T.B.) examined both eyes in rabbits and mice using a slit lamp biomicroscope (Kowa SL-15; Kowa Company, Japan) for the anterior segment and an indirect ophthalmoscope (Heine Omega 500; Heine Optotechnik, Herrsching, Germany) and lens (Volk 2.2 panretinal for rabbits, Volk 28 diopter for mice, Volk Optical; Mentor, OH) for the posterior segment. Following application of 0.5% tropicamide ophthalmic solution to both eyes, IOP was measured in rabbits using an applanation tonometer (Tono-Pen Avia; Reichert Technologies, Depew, NY).

Electroretinogram (ERG)

ERGs were performed in rabbits by a board-certified veterinary ophthalmologist (J.T.B.). Animals were dark adapted for a minimum of 1 hour prior to ERG. Animals were anesthetized using a combination of ketamine and xylazine (20–35 mg/kg and 3–5 mg/kg respectively) mixed in the syringe and delivered by intramuscular injection prior to assessment. Mydriasis was achieved with 1% tropicamide and 2.5% phenylephrine HCl applied topically to both eyes. Animals were placed in sternal recumbency with the head supported. Corneas were anesthetized by topical administration of proparacaine hydrochloride 0.5% immediately prior to the ERG exam and a wire eyelid speculum was placed. Disposable gold-foil corneal contact electrodes (ERG-Jet; Fabrisal SA, La Chaux-de-Fonda, Switzerland) were affixed to the axial corneas with coupling gel (Goniovisc Hypomellose 2.5% Ophthalmic Demulcent Solution USP, HUB Pharmaceuticals LLC, Rancho Cucamongo, CA). Disposable platinum subdermal reference and ground electrodes (Grass Technologies; Nautus Neurology, Warwick, RI) were positioned subdermally approximately 1 cm posterior to the lateral canthi bilaterally and at the occiput, respectively. Bilateral Ganzfeld domes were positioned with a camera tripod (Bogen 3021; Manfrotto Distribution, Upper Saddle River, NJ) in the direction of gaze. A stimulator unit (HM sERG; OcuScience, Henderson, NV) was used to capture simultaneous, bilateral responses under scotopic (800 mseconds recording time, 10 cd-seconds/m² stimulus intensity, 30 seconds inter-stimulus interval, 5 averages) and photopic (10 minutes light adaptation at 30 cd/m²; 800 mseconds recording time, 10 cd-seconds/m² stimulus intensity, 10 seconds inter-stimulus interval, 20 averages) conditions. Responses were low-pass filtered at 300 Hz. A forced-air warming system and warmed dry towels were used to maintain normal body temperature during recording and recovery periods. Following ERG recording, eyelid specula were removed and a sterile ocular lubricant was applied topically to prevent corneal desiccation. When xylazine reversal was required to aid in the recovery of the animal following the procedure, yohimbine or antisedan was administered subcutaneously.

Pathology

Body weights and protocol-designated organ weights were recorded for designated animals at the scheduled interim and terminal necropsies and appropriate organ weight ratios were calculated (relative to body and brain weights). Paired organs were weighed together. In rabbits, a combined weight for the thyroid and parathyroid glands was collected and only the right mandibular salivary gland was weighed. In mice, the thyroid/parathyroid gland and pituitary gland were weighed following fixation. A combined weight for the thyroid and parathyroid glands was collected, and the right mandibular/sublingual salivary glands were weighed together.

Necropsy examinations were performed under procedures approved by a board-certified veterinary pathologist. Rabbits were euthanized by an intravenous overdose of sodium pentobarbital solution followed by exsanguination by transection of the femoral vessels. Mice were euthanized by carbon dioxide inhalation followed by exsanguination by transection of the abdominal vena cava or femoral vessels. The animals were examined carefully for external abnormalities including palpable masses. The skin was reflected from a ventral midline incision and any subcutaneous masses were identified and correlated with antemortem findings. The abdominal, thoracic, and cranial cavities were examined for abnormalities. The organs were removed, examined, and, where required,

Table 2 Design of the 9-month safety study in New Zealand White rabbits and the number of animals tested at each time point for any vector dose and vehicle

Examinations	Baseline Dose (vg/eye)			2nd week Dose (vg/eye)			3rd month Dose (vg/eye)			6th month Dose (vg/eye)			9th month Dose (vg/eye)								
	2E9	2E10	2E11	2E9	2E10	2E11	2E9	2E10	2E11	2E9	2E10	2E11	2E9	2E10	2E11						
<i>In-life</i>																					
Ophthalmic examination ^a	24	24	24	28	24	24	24	24	18	18	18	21	12	12	11	13	6	6	6	6	7
IOP	24	24	24	28	24	24	24	24	18	18	18	21	12	12	11	13	6	6	6	6	7
ERG	24	24	24	28	24	24	24	24	18	18	18	21	N	N	N	N	6	6	6	6	7
Clinical pathology	24	24	24	28	24	24	24	24	18	18	18	21	12	12	12	13	6	6	6	6	7
Anti-AAV8 capsidAb	6	6	6	6	6	6	6	6	6	6	6	6	6	6	6	6	6	6	6	6	6
Anti-hRS Ab, hRS Prot.	4	4	4	4	4	4	4	4	4	4	4	4	4	4	4	4	4	4	4	4	4
Vector biodistribution ^b	24	24	24	28	24	24	24	24	18	18	18	21	12	12	12	14	6	6	6	6	7
PBMC	N	N	N	N	6	6	6	6	6	6	6	7	6	6	6	7	6	6	6	6	7
Clinical observation ^c	24	24	24	28	24	24	24	24	18	18	18	21	12	12	12	14	6	6	6	6	7
Body weight ^c	24	24	24	28	24	24	24	24	18	18	18	21	12	12	12	14	6	6	6	6	7
Food consumption ^c	24	24	24	28	24	24	24	24	18	18	18	21	12	12	12	14	6	6	6	6	7
<i>Postmortem</i>																					
Organ pathology	N	N	N	N	6	6	6	6	6	6	6	7	6	6	6	7	6	6	6	6	7
Ocular pathology	N	N	N	N	4	4	4	4	4	4	4	4	4	4	4	4	4	4	4	4	4
Vector biodistribution ^d	N	N	N	N	2	2	2	2	2	2	2	3	2	2	2	3	2	2	2	2	3

ERG, electroretinogram; IOP, intraocular pressure; N, none; PBMC, peripheral blood mononuclear cell; Veh, vehicle.

^aOphthalmic examination was performed also at 2-day postinjection in all the rabbits. ^bAnalyzed in blood samples. ^cPerformed weekly for the entire 9-month period. ^dAnalyzed in vitreous humor samples.

Table 3 Design of the 6-month safety study in Rs1-KO mice and the number of animals tested at each time point for any vector dose and vehicle

Examinations	Baseline Dose (vg/eye)			3rd day Dose (vg/eye)			1st month Dose (vg/eye)			6th month Dose (vg/eye)		
	2E9	2E10	Veh	2E9	2E10	Veh	2E9	2E10	Veh	2E9	2E10	Veh
<i>In-life</i>												
Ophthalmic examination	54	54	54	54	54	54	37	37	37	21	21	21
Clinical pathology	N	N	N	4	4	4	4	4	4	4	4	4
Anti-AAV8 capsid Ab ^b	N	N	N	5	5	5	N	N	N	9	9	8
Anti-hRS Ab, hRS protein	N	N	N	5	5	5	N	N	N	9	9	8
PBMC	N	N	N	N	N	N	4	4	4	4	4	4
Clinical observation ^a	54	54	54	54	54	54	37	37	37	21	21	21
Body weight ^a	54	54	54	54	54	54	37	37	37	21	21	21
Food consumption ^a	54	54	54	54	54	54	37	37	37	21	21	21
<i>Postmortem</i>												
Vector biodistribution	N	N	N	5	5	5	N	N	N	5	5	5
hRS gene expression	N	N	N	5	5	5	N	N	N	5	5	5
Organ pathology	N	N	N	12	12	12	12	12	12	12	12	12
Ocular pathology	N	N	N	12	12	12	12	12	12	12	12	12

N, none; PBMC, peripheral blood mononuclear cell; Veh, vehicle.

^aPerformed weekly for the entire 9-month period. ^bNot all plasma samples were analyzed for AAV8 neutralizing antibody due to hemolysis in some samples.

placed in fixative. In the mice, the pituitary was fixed *in situ*. All designated tissues were fixed in neutral buffered formalin, except for the eyes and testes, which were fixed using a modified Davidson's fixative²¹ and were placed into formalin following fixation. Formalin was infused into the lung via the trachea. A full list of tissues and organs collected from all animals are shown in Supplementary Table S4.

Microscopic examination of fixed hematoxylin and eosin-stained paraffin sections was performed on protocol-designated sections of tissues. All extraocular tissues were evaluated based on a four-step grading system (minimal, mild, moderate, severe) to define lesions for comparison between dose groups. Microscopic findings in the eyes were evaluated based on a different set of criteria, especially for inflammation.

In rabbits, an additional transverse section posterior to the first standard brain section was trimmed to include the entire optic chiasm and was embedded face down. The eyes with optic nerve (including lens) were initially fixed in modified Davidson's overnight, transferred to 10 % formalin for 24–48 hours, and subsequently processed to paraffin. The eyes were submitted for necropsy such that the left/right orientation could be identified and the superior portion of globe was marked with tissue ink. The injected (right) eye was trimmed horizontally just superior to the injection site or the optic nerve, whichever feature was most superior on the globe. The inferior trimmed portion of the globe was submitted for histological processing. A section of the lens was blocked separately from the globe (one block/one slide obtained from this tissue). The uninjected eye (left) was trimmed in the same manner as the injected eye. Green tissue dye was placed on the injection site and the uninjected eye in approximately the same location as the injection site on the right eye so that contralateral section in the approximate same locations as the injected eye could be obtained. Three sections of each eye of all designated animals were prepared from each of the following locations: area of the injection site; approximately 500 µm inferior to the injection site; two locations in the optic nerve separated by approximately 100–300 µm, and one location at least 500 µm inferior to the optic nerve. The inflammatory cells present in

different compartments of the eye were counted, rounded to the nearest ten and graded as minimal (<100), mild (100–250), moderate (250–500), and severe (>500). Hemorrhage was classified according to the number of red blood cells as minimal (<50), mild (50–100), moderate (100–150), and severe (>150). Presence of proteinaceous fluid was assessed and quantified as minimal, mild, moderate, and severe.

In mice, a total of 21 slides for each eye were generated at the time of microtomy. Two serial sections of the eye were mounted on each of the unstained slides; one section was mounted per each hematoxylin and eosin slide. The paraffin block was roughed to reveal a complete section of the eye. Three sections were obtained at this point; approximately 250 µm were roughed into the block and another three unstained slides obtained. The block was roughed again at approximately 250 µm to reach a point near, but prior to, the optic nerve, and three sections were obtained at this point. The block was roughed until the optic nerve was in plane, and three sections were obtained. The block was then step-sectioned 500 µm from the optic nerve to obtain three sections. Next, two 250-µm step-sections were taken and sections were obtained at each interval. The inflammatory cells present in different compartments of the eye were counted, rounded to the nearest ten and graded as minimal (<25), mild (25–50), moderate (50–75) and severe (>75). Hemorrhage was classified according to the number of red blood cells as minimal (<50), mild (50–100), moderate (100–150) and severe (>150). Presence of proteinaceous fluid was assessed and quantified as minimal, mild, moderate, and severe. All microscopic evaluations were performed by a board-certified veterinary pathologist (K.P.), at MPI Research, Matawan, MI, the testing facility where these two studies were conducted.

Clinical pathology

Clinical pathology evaluations were conducted on mice prior to the scheduled necropsy and on rabbits at baseline and prior to each scheduled necropsy. The animals had access to drinking water and food prior to sample

collection. At least 5 minutes prior to blood collection, rabbits were sedated with up to 1 mg/kg of acepromazine intramuscularly and blood samples (approximately 3–4 ml) were collected via the marginal ear vein from all animals. Blood samples (maximum obtainable volume) were collected from mice via the vena cava after carbon dioxide inhalation. For hematology, samples were collected in tubes containing K3EDTA; for evaluation of coagulation parameters, samples were collected in tubes containing sodium citrate; for clinical chemistry, tubes with no anticoagulant and serum separators were used. The resulting plasma samples were contained in tightly capped, pre-labeled, plastic vials and were stored frozen at -60 to -90 °C until shipped on dry ice to NIDCD, Bethesda, MD, for anticapsid antibody, anti-hRS antibody, and retinoschisin protein expression analysis. Bleeding was conducted in escalating order from the lowest to the highest vector dose group to minimize the risk of crosscontamination.

In vitro neutralization assay for AAV8

Human embryonic kidney cells, 293 cells, were maintained in Dulbecco's Modified Eagle's Medium supplemented with 10% fetal bovine serum (Atlanta Biologicals, cat # S12450) and 1% penicillin/streptomycin at 37 °C and 5% CO₂. 8E3 cells per well were seeded into 96-well plates, with 100 μ l/well medium containing full supplement. Three days later, the media were changed to 70 μ l/well fresh Dulbecco's Modified Eagle's Medium with full supplement. In a separate 96-well plate, twofold serial dilutions of the rabbit serum and mouse plasma samples were prepared, using Dulbecco's Modified Eagle's Medium supplemented with 1% penicillin/streptomycin and 1% bovine serum albumine. The dilutions ranged from 1:100 to 1:3,200 with a volume of 15 μ l in each well. 4E8/well viral genomes of AAV8-luc in an equal volume of media were added to the plasma and serum samples, incubated at 37 °C for 1 hour and then added to the 293 cells. The wells containing mixture of AAV8-luc and media without plasma or serum samples served as positive controls. Etoposide (100 μ M) was added also to each well to increase AAV transduction. The wells without AAV8-luc infection served as background controls for luciferase activity. Twenty-four hours later, luciferase activity was quantified using the One-Glo Luciferase Assay System (cat. no. E6120, Promega). The percentage of inhibition was calculated relative to positive control wells. The neutralization titer for each plasma and serum sample was defined as the plasma or serum dilution at which the relative light unit (RLU) was reduced by 50% compared with positive control wells after subtraction of the background relative light unit in nonvirus control wells.

RS1 antibody and RS1 protein detection

Enzyme-linked immunosorbent assay (ELISA) for detecting RS1 protein or anti-RS1 antibody was done on serum (rabbits) or plasma (mice, see "Biodistribution" below) samples collected from animals injected with AAV8-scRS/IRBP-hRS. The assays were performed in triplicate using standard protocols. A polyclonal anti-RS1 antibody produced in mouse (SAB1401345, Sigma-Aldrich) was employed as positive control for testing mouse plasma. A rabbit polyclonal RS1 antibody against the N terminus of RS1 (amino acid residues 24–37, translated from RS1 exons 2 and 3, (Custom Made: Thermo Fisher Scientific, Rockville, MD)) was developed and the serum collected during this stage was used as positive control. An affinity-purified guinea pig polyclonal RS1 antibody against the N terminus of retinoschisin (amino acid residues 24–37) for use in sandwich ELISA was also custom made (Project: L0930801K; Invitrogen, Carlsbad, CA). Normal mouse plasma or rabbit serum was used as a negative control (Sigma Aldrich). The specificity of antibodies to RS1 protein was tested both by western blots and immunohistochemistry using mouse retinal cell extracts. *Escherichia coli*-derived recombinant RS1 was used for generating standard curve (Cosmo Bio USA, Carlsbad, CA). For sandwich ELISA, the polyclonal RS1 antibody was biotinylated using ChromLink™ Biotin One Shot Antibody Labeling kit (Sulolink, San Diego, CA).

ELISA method to detect retinoschisin (RS1) antibodies: mouse plasma or rabbit serum with antibodies to RS1 were serially diluted and the antibodies were captured on recombinant RS1-coated ELISA plates and detected using a secondary antimouse or antirabbit antibody linked to horseradish peroxidase. The color was developed with tetramethyl benzidine (TMB). Curves of optical density (OD450) versus dilution for plasma and serum specimens were compared with positive and negative control specimens to classify the plasma and serum as positive or negative for antiretinoschisin antibodies.

Sandwich ELISA for measuring human retinoschisin (hRS1) in plasma and serum from mouse or rabbit, respectively: rabbit anti-RS1 was coated onto 96-well ELISA microtitre plates; standard recombinant RS1 or mouse plasma or rabbit serum was added and left to bind to this catching antibody; this was followed by the addition of the antirabbit RS1 antibody which has been biotinylated; finally, antibiotin conjugated to alkaline phosphatase was

added and the enzyme reaction developed and read at 405 nm. Nonlinear regression analysis was used to fit a standard curve. The concentration of RS1 protein in different plasma and serum samples was determined by standard curve created using known concentrations of *E. coli*-derived recombinant retinoschisin (RS1).

Biodistribution

In rabbits, AAV8-scRS/IRBP-hRS vector distribution was determined in blood and vitreous samples. In Rs1-KO mice, studied organs for vector biodistribution were whole blood, gonads, right epididymis, lung, heart, kidney, spleen, liver, brain, eyes, optic nerves, optic chiasm, right mandibular lymph node, right lacrimal gland, and right harderian gland. Blood was collected from rabbits from the marginal ear vein and from mice via the vena cava after carbon dioxide inhalation, as described for clinical pathology, into tubes containing K2EDTA. A portion of the whole blood from mice was centrifuged and the plasma was frozen and subsequently used for anticapsid antibodies, RS1 protein and RS1 antibodies (above). All procedures were conducted in compliance with United States Food and Drug Administration and GLP regulations. Genomic DNA was isolated and purified from the studied organs using QIAamp DNA Mini kit (Qiagen, Valencia, CA) and from the blood using QIAamp DNA Blood Mini kit (Qiagen, Valencia, CA). The concentration of DNA was determined using NanoDrop 8000 Spectrophotometer (Thermo Scientific, Waltham, MA). A TaqMan-based qPCR assay was developed and optimized to provide maximum sensitivity and specificity for detection of AAV8-scRS/IRBP-hRS vector DNA in RS1-KO mice tissues and rabbit blood and vitreous humor. 1 μ g of genomic DNA was used in triplicate to do quantitative qPCR with 2 \times TaqMan Universal Master Mix (Applied Biosystems, Waltham, MA), and the sequences of the primers to amplify hRS1 gene were 5'-TGC CAC CTC CTT GGA CTG TAT-3' and 5'-GTG ACC TCC CCT GAC TCG AA-3'; the sequence of probe was 6FAM-AGA ATG CCC ATA TCA CAA GCC TCT GGG-TAMRA-3'. The PCR conditions were set at 50 °C for 2 minutes, 95 °C for 10 minutes followed by 40 cycles of 95 °C for 15 seconds, 60 °C for 1 minute. Samples that gave results lower than 10 copies of AAV8-scRS/IRBP-hRS vector DNA per reaction were identified as "below the limit of quantitation". Samples that showed a number of copies higher than 10⁷ copies per reaction were identified as "above the limit of detection".

Rs1 gene expression analysis

Total RNA was isolated from testis, epididymis, kidney, heart, spleen, lung, mandibular lymphnode, liver, brain, harderian, and lacrimal gland tissues of Rs1-KO mice using RNAeasy mini kit (Qiagen) following the manufacturer instruction. Isolated RNA samples were analyzed using NanoDrop 8000 Spectrophotometer and Agilent 2100 Bioanalyzer to insure the integrity of RNA. Total RNA (100ng) from each tissue was reverse transcribed to cDNA using oligo (dT) and high-capacity cDNA reverse transcription kit (Applied Biosystems). A TaqMan-based qPCR assay was developed and optimized to provide maximum sensitivity and specificity for detection of hRS1 RNA in AAV8-scRS/IRBP-hRS-dosed Rs1-KO mice. One tenth of reverse-transcribed product was used in triplicates to do qPCR with 2 \times TaqMan Universal Master Mix (Applied Biosystems), and the sequences of the primers to amplify hRS1 gene were 5'-TGT CAC GCA AGA TAG AAG GC-3' and 5'-CCT TCA TCC TCG GTA GAC GAT A-3', which amplifies an 85-bp fragment from the junction region of exons 1 and 3 of hRS1 cDNA and, therefore, specific to hRS1 RNA in AAV8-scRS/IRBP-hRS-dosed Rs1-KO mice, but will not react with mouse tissue DNA and viral vector genomic DNA. The sequence of probe was 5'-6FAM-TCT TTG GCT ATG AAG CCA CAT TGG GA-MGB-3'. The PCR conditions were set at 50 °C for 2 minutes, 95 °C for 10 minutes followed by 40 cycles of 95 °C for 15 seconds, 60 °C for 1 minute. The procedure of qPCR was validated as following: five runs of the qPCR assay of pAAVscRSIRBP hRS plasmid DNA were performed by two operators to determine the performance characteristics across 5 days. The sensitivity and the linear range of the optimized assay were evaluated from the standard curves run in the five validation tests. Each standard curve was analyzed for limit of detection, lower limit of quantification, upper limit of quantification, slope of the standard curve, amplification efficiency (E), Y-intercepts, and correlation coefficients (R²). Different lots of PCR master mix, primers, and probes were used during the five assays to test their effect on assay variation. The intra- and interassay precision and accuracy were evaluated using three levels of quality control (QC) samples prepared and tested separately in the five validation runs. Two sets of QC samples were separately prepared at the same time the standard curve was prepared for each of the five qPCR assays. Therefore, each assay was run with two QC sets and a total of six reactions at each QC concentration. The two sets of QC samples, 18 reactions in total, were tested on the same 96-well plate with the standard curve. Tests of ten QC sets were finished on five plates in 5 days with two sets being analyzed on one plate per day.

Measurement of viral capsid and transgene-specific lymphocyte proliferation and IFN γ -producing T-cell responses

Rabbit PBMCs were isolated from whole blood by sucrose gradient. After isolation, the cells were washed and red blood cells were lysed. PBMCs were then labeled with a carboxyfluorescein diacetate succinimidyl ester staining solution, and placed into culture medium. PBMCs were cultured under five separate conditions: a solution of non-AAV8 peptides which served as a negative control, concanavalin A stimulation solution as the positive control, and three separate AAV8 PP for 6 days (media and peptides replaced after 3 days of culture). The AAV8 capsid peptide library of 182 peptides (peptide purity >80 %) was generated as 15mers overlapping 11 amino acids (Mimotopes, Victoria Australia). For AAV-8 capsid, three PP were created: PP1 (peptides 1–60), PP2 (peptides 61–120), and PP3 (peptides 121–182). Peptides were pooled such that the final concentration of each peptide in any given pool was 170 $\mu\text{g}/\text{ml}$. After culture, the cells were then stained for viability marker (Zombie dye) and then fixed with IO Test™ 3. The prepared specimens were analyzed on a LSR Fortessa flow cytometer with FACS Diva software for the carboxyfluorescein diacetate succinimidyl ester and viability dye markers on the cytometer. For each sample, the gating was adjusted in relation to the negative control to compensate for interanimal variance within the assay.

Mice were euthanized and their spleens were excised and lymphocytes harvested. Mouse spleen lymphocytes were cultured in seven separate conditions; negative control, a phorbol 12-myristate 13-acetate and ionomycin stimulation solution which was utilized as the positive control, and PP (three AAV8 and two RS1 PP (Proimmune Inc., Oxford, UK)) for 6 hours. After culture, the cells were then washed and stained for inter and extracellular markers to assess T-cell activity. Aliquots of the spleen specimens were stained with predetermined volumes of previously tested and titered monoclonal antibodies specific for each phenotype marker. Before staining, the red blood cells in each sample were lysed. Samples were fixed during the intracellular antibody staining process with BD Perm/Fix buffer solution. The prepared specimens were analyzed on a LSR Fortessa flow cytometer with FACS Diva software. *In vitro* T-cell mediated immune responses were monitored via percent of CD3+CD45+CD4+IFN γ + and CD3+CD45+CD8+IFN γ + of CD45+CD3+ cells. For each specimen, percentages values were calculated independently per phenotype.

Statistical analysis

For each of the following endpoints (body weights, food consumption, hematology (except leukocyte counts), clinical chemistry, organ weights, interocular ratio in ERG amplitude and IOP values), treatment groups (AAV8-vector injected animals) were compared with the control group (vehicle-injected animals) by group pair-wise comparisons. Since leukocyte counts (total and differential) are not normally distributed, a log transformation was performed on these data prior to group pair-wise comparisons. Where sample sizes for all groups were three or greater, Levene's test²² was used to assess homogeneity of group variances for each specified endpoint and for all collection intervals. If Levene's test was not significant ($P \geq 0.01$), a pooled estimate of the variance (mean square error or MSE) was computed from a one-way analysis of variance (ANOVA) and utilized by a Dunnett's comparison²³ of each treatment group with the control group. If Levene's test was significant ($P < 0.01$), comparisons with the control group were made using Welch's *t*-test²⁴ with a Bonferroni correction. Where the sample was less than three for at least one treatment group, Levene's method could not be implemented. Groups with sample sizes less than three were excluded from the analysis, and control to treatment pair-wise comparisons that satisfied the sample size assumption ($n \geq 3$) were conducted using Welch's *t*-test with a Bonferroni correction. Results of all pair-wise comparisons are reported at the 0.05 and 0.01 significance levels. All endpoints were analyzed using two-tailed tests unless indicated otherwise.

ACKNOWLEDGMENTS

This study was supported by the Intramural Research Program of the National Eye Institute and National Institute on Deafness and Other Communication Disorders.

REFERENCES

1. Sauer, CG, Gehrig, A, Warneke-Wittstock, R, Marquardt, A, Ewing, CC, Gibson, A et al. (1997). Positional cloning of the gene associated with X-linked juvenile retinoschisis. *Nat Genet* **17**: 164–170.

2. Gehrig, AE, Warneke-Wittstock, R, Sauer, CG and Weber, BH (1999). Isolation and characterization of the murine X-linked juvenile retinoschisis (Rs1h) gene. *Mamm Genome* **10**: 303–307.
3. Sieving, PA, MacDonald, IM, and Chan, S (1993). X-linked juvenile retinoschisis. In: Pagon, RA, et al. (eds). *GeneReviews(R)*. Univ. of Washington: Seattle, WA.
4. Tantri, A, Vrabec, TR, Cu-Unjieng, A, Frost, A, Annesley, WH Jr and Donoso, LA (2004). X-linked retinoschisis: a clinical and molecular genetic review. *Surv Ophthalmol* **49**: 214–230.
5. Sikkink, SK, Biswas, S, Parry, NR, Stanga, PE and Trump, D (2007). X-linked retinoschisis: an update. *J Med Genet* **44**: 225–232.
6. Zeng, Y, Takada, Y, Kjellstrom, S, Hiriyanna, K, Tanikawa, A, Wawrousek, E et al. (2004). RS-1 gene delivery to an adult Rs1h knockout mouse model restores ERG b-wave with reversal of the electronegative waveform of X-linked retinoschisis. *Invest Ophthalmol Vis Sci* **45**: 3279–3285.
7. Kjellstrom, S, Bush, RA, Zeng, Y, Takada, Y and Sieving, PA (2007). Retinoschisis gene therapy and natural history in the Rs1h-KO mouse: long-term rescue from retinal degeneration. *Invest Ophthalmol Vis Sci* **48**: 3837–3845.
8. Park, TK, Wu, Z, Kjellstrom, S, Zeng, Y, Bush, RA, Sieving, PA et al. (2009). Intravitreal delivery of AAV8 retinoschisin results in cell type-specific gene expression and retinal rescue in the Rs1-KO mouse. *Gene Ther* **16**: 916–926.
9. Min, SH, Molday, LL, Seeliger, MW, Dinculescu, A, Timmers, AM, Janssen, A et al. (2005). Prolonged recovery of retinal structure/function after gene therapy in an Rs1h-deficient mouse model of x-linked juvenile retinoschisis. *Mol Ther* **12**: 644–651.
10. Janssen, A, Min, SH, Molday, LL, Tanimoto, N, Seeliger, MW, Hauswirth, WW et al. (2008). Effect of late-stage therapy on disease progression in AAV-mediated rescue of photoreceptor cells in the retinoschisin-deficient mouse. *Mol Ther* **16**: 1010–1017.
11. Byrne, LC, Oztürk, BE, Lee, T, Fortuny, C, Visel, M, Dalkara, D et al. (2014). Retinoschisin gene therapy in photoreceptors, Müller glia or all retinal cells in the Rs1h^{-/-} mouse. *Gene Ther* **21**: 585–592.
12. Ou, J, Vijayarathay, C, Ziccardi, L, Chen, S, Zeng, Y, Marangoni, D et al. (2015). Synaptic pathology and therapeutic repair in adult retinoschisis mouse by AAV-RS1 transfer. *J Clin Invest* **125**: 2891–2903.
13. Marangoni, D, Wu, Z, Wiley, HE, Zeiss, CJ, Vijayarathay, C, Zeng, Y et al. (2014). Preclinical safety evaluation of a recombinant AAV8 vector for X-linked retinoschisis after intravitreal administration in rabbits. *Hum Gene Ther Clin Dev* **25**: 202–211.
14. Leberher, C, Maguire, A, Tang, W, Bennett, J and Wilson, JM (2008). Novel AAV serotypes for improved ocular gene transfer. *J Gene Med* **10**: 375–382.
15. Jacobson, SG, Boye, SL, Aleman, TS, Conlon, TJ, Zeiss, CJ, Roman, AJ et al. (2006). Safety in nonhuman primates of ocular AAV2-RPE65, a candidate treatment for blindness in Leber congenital amaurosis. *Hum Gene Ther* **17**: 845–858.
16. Maclachlan, TK, Lukason, M, Collins, M, Munger, R, Isenberger, E, Rogers, C et al. (2011). Preclinical safety evaluation of AAV2-sFLT01—a gene therapy for age-related macular degeneration. *Mol Ther* **19**: 326–334.
17. Koilkonda, RD, Yu, H, Talla, V, Porciatti, V, Feuer, WJ, Hauswirth, WW et al. (2014). LHON gene therapy vector prevents visual loss and optic neuropathy induced by G11778A mutant mitochondrial DNA: biodistribution and toxicology profile. *Invest Ophthalmol Vis Sci* **55**: 7739–7753.
18. Koilkonda, RD, Yu, H, Chou, TH, Feuer, WJ, Ruggeri, M, Porciatti, V et al. (2014). Safety and effects of the vector for the Leber hereditary optic neuropathy gene therapy clinical trial. *JAMA Ophthalmol* **132**: 409–420.
19. Jager, RD, Aiello, LP, Patel, SC and Cunningham, ET Jr (2004). Risks of intravitreal injection: a comprehensive review. *Retina* **24**: 676–698.
20. Nakano, T, Hasegawa, K, Tomatsu, M and Muto, H (1990). Postnatal transformation and location of mitoses in the epithelium lining the mouse vomeronasal organ. *Okajimas Folia Anat Jpn* **67**: 81–88.
21. Latendresse, JR, Warbritton, AR, Jonassen, H and Creasy, DM (2002). Fixation of testes and eyes using a modified Davidson's fluid: comparison with Bouin's fluid and conventional Davidson's fluid. *Toxicol Pathol* **30**: 524–533.
22. Milliken, GA and Johnson, DE (1992). *Analysis of Messy Data*. Chapman and Hall: London. pp. 21–29.
23. Dunnett, CW (1955). A multiple comparison procedure for comparing several treatments with a control. *J Am Stat Assoc* **50**: 1096–1121.
24. Welch, BL (1937). The significance of difference between two means when the population variances are unequal. *Biometrika* **29**: 350–362.



This work is licensed under a Creative Commons Attribution-NonCommercial-NoDerivs 4.0 International License. The images or other third party material in this article are included in the article's Creative Commons license, unless indicated otherwise in the credit line; if the material is not included under the Creative Commons license, users will need to obtain permission from the license holder to reproduce the material. To view a copy of this license, visit <http://creativecommons.org/licenses/by-nc-nd/4.0/>

Supplementary Information accompanies this paper on the *Molecular Therapy—Methods & Clinical Development* website (<http://www.nature.com/mtm>)